

# Synthesis and Fluorescence Quantum Yield of $Gd_{1-x}Eu_xOOH$ Crystals

Hiroaki Samata<sup>1</sup>, Daisuke Itakura<sup>1</sup>, Shungo Imanaka<sup>1</sup>, Tadashi C. Ozawa<sup>2</sup>

<sup>1</sup>Graduate School of Maritime Sciences, Kobe University, Kobe, Japan

<sup>2</sup>International Center for Materials Nanoarchitectonics, National Institute for Materials Science, Tsukuba, Japan

Email: [samata@maritime.kobe-u.ac.jp](mailto:samata@maritime.kobe-u.ac.jp)

Received 4 February 2014; revised 4 March 2014; accepted 11 March 2014

Copyright © 2014 by authors and Scientific Research Publishing Inc.

This work is licensed under the Creative Commons Attribution International License (CC BY).

<http://creativecommons.org/licenses/by/4.0/>



Open Access

---

## Abstract

$Eu^{3+}$ -doped gadolinium oxyhydroxide  $Gd_{1-x}Eu_xOOH$  crystals were synthesized by the flux method. The X-ray diffraction data for the crystals were well refined assuming a monoclinic structure with the  $P2_1/m$  space group.  $Gd_{1-x}Eu_xOOH$  ( $x \leq 0.2$ ) crystals showed strong red emission, and the highest fluorescence quantum yield ( $\Phi_f$ ) was 0.27, obtained for  $x = 0.10$ .  $\Phi_f$  decreased rapidly as the  $Eu^{3+}$  content  $x$  increased above 0.2, owing to concentration quenching. Analysis with a percolation model indicated three-dimensional energy transfer between the  $Eu^{3+}$  ions.

## Keywords

Gadolinium Oxyhydroxide; Fluorescence Quantum Yield; Percolation Model

---

## 1. Introduction

Some rare-earth compounds have excellent optical properties and hence are widely used in high-performance luminescence devices and as catalyst supports. Trivalent rare-earth ions such as  $Eu^{3+}$ ,  $Tb^{3+}$ , and  $Tm^{3+}$ -doped in a suitable host material show strong emission based on electron transition between the  $4f$  orbitals. The luminescence properties depend strongly on the chemical composition and crystal structure of the host material. One of the Gd(III) compounds, gadolinium oxyhydroxide ( $GdOOH$ ), which has a monoclinic structure with the  $P2_1/m$  space group, can be obtained as a stable phase by the thermal dehydration of hydroxide  $Gd(OH)_3$  [1]-[4]. Although this compound can function as a host material for phosphors, there are very few reports on its photoluminescence properties [5] [6]. Fluorescence quantum yield,  $\Phi_f$ , which is defined as the ratio of the number of emitted photons to the number of absorbed photons, is a fundamental parameter that decides the photoluminescence efficiency of a compound/phosphor [7]. Hence, evaluation of the activator content dependence of  $\Phi_f$  using high-quality single-crystal specimens is important.

In this study, we synthesized  $\text{Gd}_{1-x}\text{Eu}_x\text{OOH}$  crystals and evaluated their luminescence properties, including  $\Phi_f$ . In addition, we evaluated the critical  $\text{Eu}^{3+}$  concentration in the  $\text{Gd}_{1-x}\text{Eu}_x\text{OOH}$  system by using a percolation model.

## 2. Experimental

Crystals of  $\text{Eu}^{3+}$ -doped gadolinium oxyhydroxide,  $\text{Gd}_{1-x}\text{Eu}_x\text{OOH}$  ( $x = 0, 0.02, 0.04, 0.06, 0.08, 0.1, 0.15, 0.2, 0.3, 0.4, 0.5, 0.6, 0.8, 1$ ), were synthesized by the flux method. Appropriate amounts of  $\text{Gd}_2\text{O}_3$  powder (99.9%) and  $\text{Eu}_2\text{O}_3$  powder (99.9%) were mixed in an agate mortar for 1 h. Then, the  $\text{Gd}_2\text{O}_3/\text{Eu}_2\text{O}_3$  mixture was placed in a 20-mL Zr crucible and covered by a layer of a NaOH (15 g)/KOH (5 g) mixture. The crucible was placed in an alumina container, covered with an alumina lid, and heated in an electric furnace at  $330^\circ\text{C}$  for 72 h in ambient atmosphere. Subsequently, the flux was dissolved in large excess of water; the obtained crystals were washed thoroughly in distilled water to remove any residual flux and dried on a hot plate at  $80^\circ\text{C}$  for 1 h.

The chemical composition of the crystals was measured using an inductively coupled plasma optical emission spectrometer (ICP-OES; Seiko Instruments Inc., SPS1700HVR) and an energy-dispersive X-ray spectrometer (EDS; JEOL, EX-23000 BU). The crystal structures were identified by powder X-ray diffraction (XRD; Rigaku, RINT2000). The diffraction data were acquired using  $\text{CuK}\alpha$  radiation generated at 40 kV and 20 mA, in the  $2\theta$  range  $10\text{--}80^\circ$  at room temperature, and refined by the Rietveld method [8]. Thermogravimetric analysis (TG) and differential thermal analysis (DTA) were carried out in air, at temperatures between 30 and  $785^\circ\text{C}$  at a heating rate of  $10^\circ\text{C}/\text{min}$  (Seiko Instruments Inc., TG/DTA6300). The fluorescence excitation and emission spectra were measured at room temperature using a fluorescence spectrophotometer (Hitachi, F-7000). The excitation spectra were corrected for the spectral distribution of the lamp intensity by the Rhodamine B method, and the emission spectra were corrected for the spectral response of the instrument by using a substandard light source. The  $\Phi_f$  values were measured using an absolute photoluminescence quantum yield measurement system (Hamamatsu, C9920-02), at room temperature [7].

## 3. Results and Discussion

$\text{Gd}_{1-x}\text{Eu}_x\text{OOH}$  crystallized at the bottom of the crucible. As shown in **Figure 1**, the as-grown  $\text{GdOOH}$  crystals were transparent and had a plate-like shape with flat surfaces, which could be attributed to the growth in a liquid phase. The maximum length of the crystal was about 1.2 mm. The external surface of the crystals remained largely unchanged through the entire composition range. No trace of Zr, Na, and K impurities was detected by ICP-OES measurements, although these elements were expected to be incorporated into the crystals because of the use of the Zr crucible and NaOH/KOH mixture. The Gd/Eu ratio in the grown crystals, which was measured by EDS, was in good agreement with the molar ratios of  $\text{Gd}_2\text{O}_3$  and  $\text{Eu}_2\text{O}_3$ , indicating that  $\text{Gd}_{1-x}\text{Eu}_x\text{OOH}$  crystals with different compositions could be obtained by simply changing the molar ratio of the starting materials.

**Figure 2** shows the powder XRD profiles of  $\text{Gd}_{1-x}\text{Eu}_x\text{OOH}$  and the result of data refinement by the Rietveld method. The black squares show the experimental data, and the red and blue solid lines show the calculated profile and the difference between the experimental and calculated profiles, respectively. All the diffraction data were well refined assuming a monoclinic structure with the  $P2_1/m$  space group, and no structural change was observed over the entire composition range considered. The lattice parameters for  $\text{GdOOH}$  ( $a = 0.4339$  nm,  $b = 0.3717$  nm,  $c = 0.6072$  nm,  $\beta = 108.79^\circ$ ) and  $\text{EuOOH}$  ( $a = 0.4346$  nm,  $b = 0.3744$  nm,  $c = 0.6107$  nm,  $\beta = 108.62^\circ$ ) agreed with those reported in previous studies [9] [10]. When  $\text{Gd}^{3+}$  (ionic radius: 0.0935 nm) in  $\text{GdOOH}$  was replaced by  $\text{Eu}^{3+}$  (ionic radius: 0.0947 nm), the lattice constants showed a slight increase, in accordance with Vegard' law.  $\text{Gd}_{1-x}\text{Eu}_x\text{OOH}$  had low rare-earth site symmetry and a layered structure in which the rare earth layers were sandwiched between an O layer and an OH layer [11] [12].

The TG curve of the as-grown crystals indicated no apparent weight loss in the temperature range  $30\text{--}400^\circ\text{C}$ , indicating that the as-grown crystals did not include  $\text{Gd}(\text{OH})_3$ , which normally decomposes at  $270^\circ\text{C}$  [4]. In the TG profile, the first large weight loss was observed at  $445^\circ\text{C}$ , with a corresponding endothermic effect, attributable to the removal of water molecules from  $\text{GdOOH}$  crystals. The experimental weight loss of 4.5% agreed well with the theoretical value of 4.7% calculated assuming the following thermal decomposition:  $2\text{GdOOH} \rightarrow \text{Gd}_2\text{O}_3 + \text{H}_2\text{O}$ . The XRD profiles of the specimens subjected to TG/DTA measurements showed a single phase,  $\text{Gd}_2\text{O}_3$ . These results indicated that the as-grown crystals comprised a single phase of  $\text{GdOOH}$  and did not contain  $\text{Gd}_2\text{O}_3$  and  $\text{Gd}(\text{OH})_3$  at all.

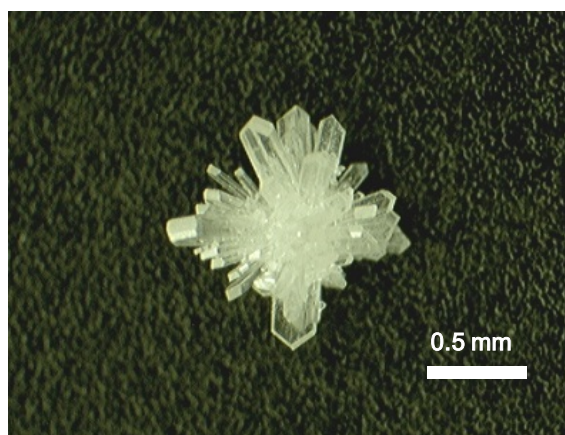


**Figure 1.** Photograph of as-grown GdOOH crystals synthesized at 330°C for 72 h.

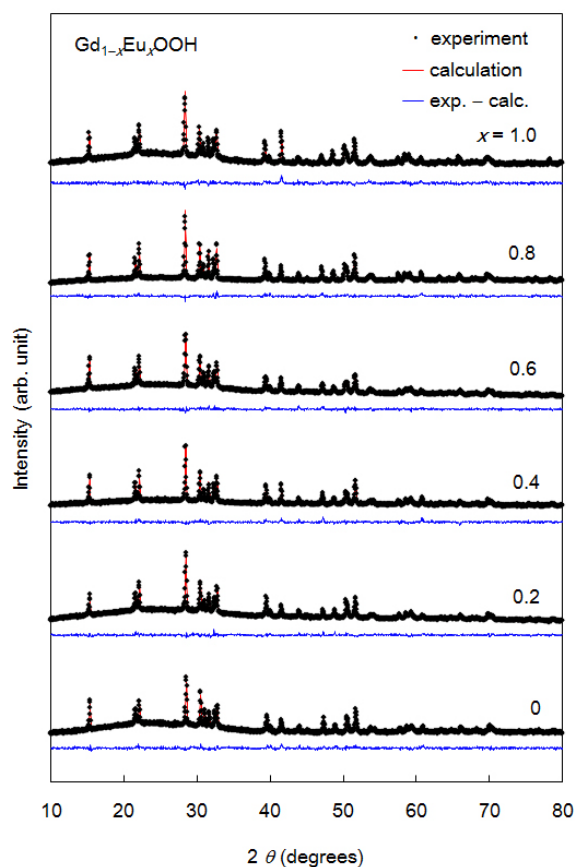


**Figure 2.** Powder X-ray diffraction profiles of  $Gd_{1-x}Eu_xOOH$  crystals and results of data refinement by the Rietveld method.

**Figure 3** shows the excitation spectra of the  $Gd_{1-x}Eu_xOOH$  crystals; spectral measurements were performed at 617 nm, which is the maximum emission wavelength of  $Eu^{3+}$  in this system ( ${}^5D_0 \rightarrow {}^7F_2$  transition). The excitation spectra showed sharp peaks between 300 nm and 550 nm, which were attributed to the direct intraconfigurational  $4f-4f$  transitions from the  ${}^7F_0$  and  ${}^7F_1$  levels of  $Eu^{3+}$ . The intensity of these peaks increased as the  $Eu^{3+}$  content increased up to  $x = 0.1$ . The wide peak between 200 nm and 300 nm, which was attributed to the overlapping of

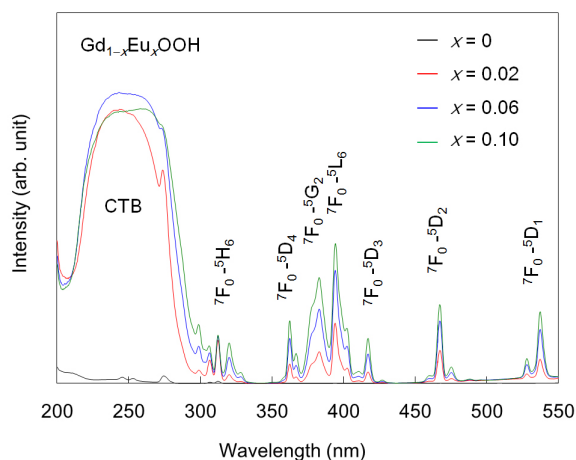


**Figure 3.** Excitation spectra of  $Gd_{1-x}Eu_xOOH$  crystals.

the  $O^{2-}$  to  $Eu^{3+}$  charge transfer band (CTB) and the band due to energy transfer from  $Gd^{3+}$  to  $Eu^{3+}$  [13], indicated energy transfer from the oxyhydroxide host to  $Eu^{3+}$ . The intensity of the sharp peaks appearing at wavelengths longer than 300 nm changed with the  $Eu^{3+}$  content, but that of the wide peak at wavelengths below 300 nm did not change much.

**Figure 4** shows the emission spectrum of the  $Gd_{0.9}Eu_{0.1}OOH$  crystals under 243 nm illumination. Strong red luminescence from  $Eu^{3+}$  was observed in the visible range. These peaks could be attributed to the transition from the lowest excited level  $^5D_0$  to the  $^7F_{0-4}$  levels of the ground term. The most intense transition was  $^5D_0 \rightarrow ^7F_2$ , the allowed electric dipole transition, at 617 nm. The other electric dipole transition,  $^5D_0 \rightarrow ^7F_4$ , was observed near 710 nm. In addition to electric dipole transitions, a strong magnetic dipole transition,  $^5D_0 \rightarrow ^7F_1$ , was observed near 595 nm. A  $^5D_0 \rightarrow ^7F_0$  transition, which is normally forbidden by the free-ion selection rules, occurred at around 580 nm, as the selection rules are broken by the low symmetry of the rare-earth sites.

**Figure 5** shows the  $Eu^{3+}$  content dependence of  $\Phi_f$  for the  $Gd_{1-x}Eu_xOOH$  crystals under excitation at 243, 258, and 394 nm ( $Eu^{3+}: ^7F_0 \rightarrow ^5L_6$ ), with the former two wavelengths being close to the peak maxima in the excitation spectra. The highest  $\Phi_f$  of 0.27 was obtained when the  $Eu^{3+}$  content was around 0.1. The decrease in  $\Phi_f$  for  $x < 0.1$  was attributed to the small amount of  $Eu^{3+}$ , which is the photoactivator, in the system. At all excitation wavelengths,  $\Phi_f$  decreased rapidly as the  $Eu^{3+}$  content increased beyond 0.2, because of concentration quenching caused by the transfer of excitation energy between the  $Eu^{3+}$  ions.

The critical  $Eu^{3+}$  concentration was evaluated by using the percolation model, which has been used to explain energy transfer in the solid state [14]–[16]. In this study, the aforesaid model was applied to the system under the following assumptions: energy transfer between the  $Eu^{3+}$  ions occurs only among the neighbor sites in the rare-earth sublattice. When the  $Eu^{3+}$  concentration was below the critical value, the  $Eu^{3+}$  ions showed emission individually, and the  $\Phi_f$  values were high. When the  $Eu^{3+}$  concentration exceeded the critical value  $P_c$ ,  $\Phi_f$  decreased rapidly because of energy transfer from the percolating cluster to the killer center, which consists of vacancies and impurities. V. A. Vyssotsky *et al.* suggested the following expression for calculating the critical concentration in the percolation model:

$$P_c = d/z(d-1) \quad (1)$$

where  $P_c$ ,  $z$ , and  $d$  are the critical concentration, number of neighbor sites, and number of dimensions, respectively [16]. When energy transfer between the  $Eu^{3+}$  ions occurs only in the inner layers of the rare-earth sublattice, the number of dimensions is considered to be 2 (pseudo-two-dimensional energy transfer). When energy transfer occurs in the interlayers, the number of dimensions is considered to be 3 (three-dimensional energy transfer). **Figure 6** shows the percolation model and the  $P_c$  value calculated using Equation (1). In this figure, only the rare-earth sublattice is depicted, and the  $Eu^{3+}$  ions between which energy transfer occurs are bonded by gray cylinders. Energy transfer between the  $Eu^{3+}$  ions is assumed to occur within 0.363 nm for (a), 0.373 nm for (b), 0.404 nm for (c), and 0.435 nm for (d). The experimental result agrees well with the calculated value of  $P_c$  (0.19) estimated for  $Eu^{3+}$ - $Eu^{3+}$  interactions within 0.404 nm (c). In this case, the  $Eu^{3+}$  ions have eight neighbors

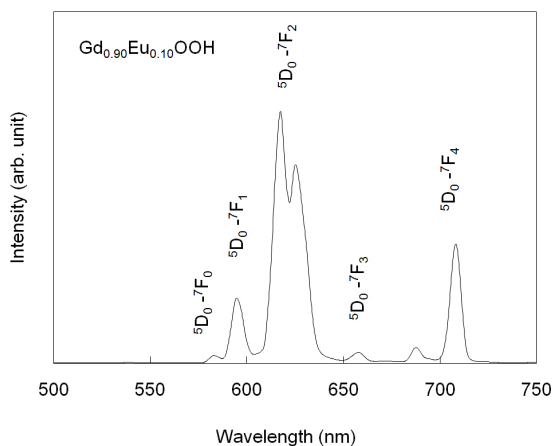


Figure 4. Emission spectrum of  $Gd_{0.9}Eu_{0.1}OOH$  crystals.

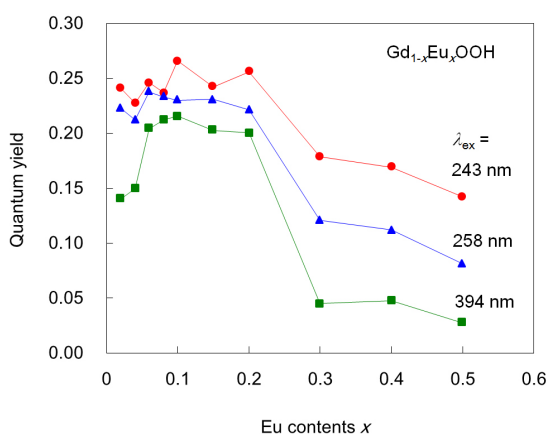


Figure 5.  $Eu^{3+}$  content dependence of the fluorescence quantum yield  $\Phi_f$  of  $Gd_{1-x}Eu_xOOH$  crystals.

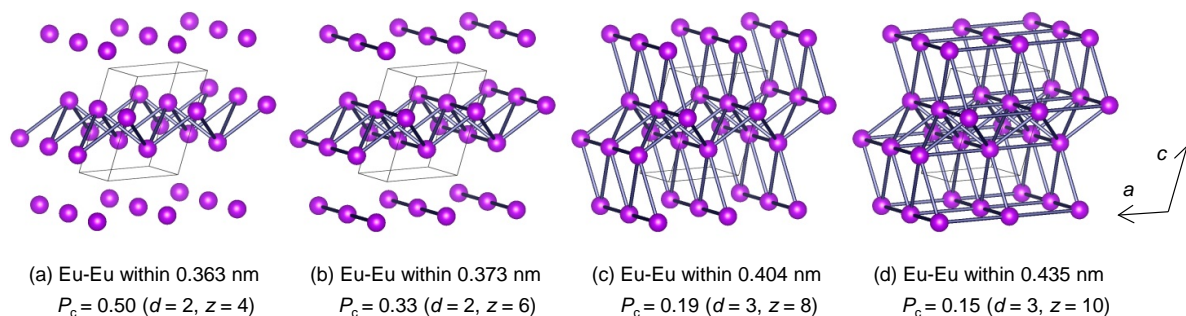


Figure 6. Percolation model of the  $Gd_{1-x}Eu_xOOH$  system.

with three-dimensional energy transfer. This result indicates three-dimensional energy transfer occurs between the  $Eu^{3+}$  ions in this system.

To improve the luminescence properties of the crystals, it is necessary to increase the critical concentration of  $Eu^{3+}$ . In general, compounds with a low-dimensional arrangement of rare-earth ions show a high critical concentration. On the basis of the results obtained using the percolation model in this study, we state that two-dimensional models have a higher critical concentration (0.50 and 0.33) than do three-dimensional models. When the increase in the distance between the rare-earth layers restrains interlayer energy transfer, the critical concentration of  $Eu^{3+}$  in this system can increase. Therefore, excellent luminescence properties can be obtained by co-doping larger ions in the rare-earth sublattice with a high level of  $Eu^{3+}$  doping. The high alkali durability of

the  $\text{Gd}_{1-x}\text{Eu}_x\text{OOH}$  crystals is confirmed by the fact that they are stable in NaOH/KOH solution at 330°C.

#### 4. Conclusion

$\text{Gd}_{1-x}\text{Eu}_x\text{OOH}$  crystals with a maximum length of 1.2 mm were synthesized by the flux method. The  $\text{Gd}_{1-x}\text{Eu}_x\text{OOH}$  ( $x \leq 0.2$ ) crystals showed strong red emission, with the maximum  $\Phi_f$  of 0.27 for  $x = 0.10$ . The critical  $\text{Eu}^{3+}$  content was 0.2, because  $\Phi_f$  decreased rapidly beyond this level owing to concentration quenching. This critical content was the closest to that estimated by a percolation model for  $\text{Eu}^{3+}$ - $\text{Eu}^{3+}$  interactions within 0.404 nm, wherein  $\text{Eu}^{3+}$  had eight neighbors, indicating three-dimensional energy transfer between the  $\text{Eu}^{3+}$  ions in the rare-earth sublattice. The synthesized crystals showed excellent alkali durability and hence may be used as a high-efficiency host material in unique photomedical applications such as photochemical internalization and photodynamic therapy.

#### Acknowledgements

This study was supported by JSPS KAKENHI Grant Number 21560696, 24560827.

#### References

- [1] Klevtsov, P.V. and Sheina, L.P. (1965) Hydrothermal Synthesis and Crystal Structure of Rare-Earth Hydroxides. *Izvestiya Akademii Nauk SSSR, Neorganicheskie Materialy*, **1**, 912.
- [2] Klevtsov, P.V. and Sheina, L.P. (1965) Thermographic and X-ray Studies of Crystalline Hydroxides of the Rare Earth Elements. *Izvestiya Akademii Nauk SSSR, Neorganicheskie Materialy*, **1**, 2219.
- [3] Gondrand, M. and Christensen, A.N. (1971) Hydrothermal and High Pressure Preparation of Some Rare Earth Trihydroxides and Some Rare Earth Oxide Hydroxides. *Materials Research Bulletin*, **6**, 239-246. [http://dx.doi.org/10.1016/0025-5408\(71\)90036-5](http://dx.doi.org/10.1016/0025-5408(71)90036-5)
- [4] Yamamoto, O., Takeda, Y., Kanno, R. and Fushimi, M. (1985) Thermal Decomposition and Electrical Conductivity of  $\text{M}(\text{OH})_3$  and  $\text{MOOH}$  ( $M=Y$ , Lanthanide). *Solid State Ionics*, **17**, 107-114. [http://dx.doi.org/10.1016/0167-2738\(85\)90057-8](http://dx.doi.org/10.1016/0167-2738(85)90057-8)
- [5] Hölsä, J., Leskelä, T. and Leskelä, M. (1985) Luminescence Properties of Europium(3+)-Doped Rare-Earth Oxyhydroxides. *Inorganic Chemistry*, **24**, 1539-1542. <http://dx.doi.org/10.1021/ic00204a026>
- [6] Hölsä, J. (1990) Simulation of Crystal Field Effect in Monoclinic Rare Earth Oxyhydroxides Doped with Trivalent Europium. *The Journal of Physical Chemistry*, **94**, 4835-4838. <http://dx.doi.org/10.1021/j100375a016>
- [7] Suzuki, K., Kobayashi, A., Kaneko, S., Takehira, K., Yoshihara, T., Ishida, H., Shiina, Y., Oishic, S. and Tobita, S. (2009) Reevaluation of Absolute Luminescence Quantum Yields of Standard Solutions Using a Spectrometer with an Integrating Sphere and a Back-Thinned CCD Detector. *Physical Chemistry Chemical Physics*, **11**, 9850-9860. <http://dx.doi.org/10.1039/b912178a>
- [8] Izumi, F. and Ikeda, T. (2000) A Rietveld-Analysis Programm RIETAN-98 and Its Applications to Zeolites. *Materials Science Forum*, **321-324**, 198-205. <http://dx.doi.org/10.4028/www.scientific.net/MSF.321-324.198>
- [9] Chang, C. and Mao, D. (2006) Thermal Dehydration Kinetics of a Rare Earth Hydroxide,  $\text{Gd}(\text{OH})_3$ . *International Journal of Chemical Kinetics*, **39**, 75-81. <http://dx.doi.org/10.1002/kin.20221>
- [10] Bärnighausen, V. H. (1965) Die Elementarzelle und Raumgruppe von  $\text{EuOOH}$ . *Acta Crystallographica*, **19**, 1047.
- [11] Samata, H., Kimura, D., Mizusaki, S., Nagata, Y., Ozawa, T.C. and Sato, A. (2009) Synthesis and Characterization of Neodymium Oxyhydroxide Crystals. *Journal of Alloys and Compounds*, **468**, 566-570. <http://dx.doi.org/10.1016/j.jallcom.2008.01.056>
- [12] Samata, H., Kimura, D., Saeki, Y., Nagata, Y. and Ozawa, T.C. (2007) Synthesis of Lanthanum Oxyhydroxide Single Crystals Using an Electrochemical Method. *Journal of Crystal Growth*, **304**, 448-451. <http://dx.doi.org/10.1016/j.jcrysgro.2007.03.025>
- [13] Yang, J., Li, C., Cheng, Z., Zhang, X., Quan, Z., Zhang, C. and Lin, J. (2007) Size-Tailored Synthesis and Luminescent Properties of One-Dimensional  $\text{Gd}_2\text{O}_3:\text{Eu}^{3+}$  Nanorods and Microrods. *The Journal of Physical Chemistry C*, **111**, 18148-18154. <http://dx.doi.org/10.1021/jp0767112>
- [14] Vyssotsky, V.A., Gordon, S.B., Frisch, H.L. and Hammersley, J.M. (1961) Critical Percolation Probabilities (Bond Problem). *Physical Review*, **123**, 1566. <http://dx.doi.org/10.1103/PhysRev.123.1566>
- [15] Keyes, K. and Pratt, S. (1979) The Relation of Percolation to Energy Migration Dynamics. *Chemical Physics Letters*,

- 65, 100-104. [http://dx.doi.org/10.1016/0009-2614\(79\)80136-0](http://dx.doi.org/10.1016/0009-2614(79)80136-0)
- [16] Honma, T., Toda, K., Ye, Z.G. and Sato, M. (1998) Concentration Quenching of the  $\text{Eu}^{3+}$ -Activated Luminescence in Some Layered Perovskites with Two-Dimensional Arrangement. *The Journal of Physical Chemistry of Solids*, **59**, 1187-1193. [http://dx.doi.org/10.1016/S0022-3697\(98\)00056-0](http://dx.doi.org/10.1016/S0022-3697(98)00056-0)